The Influence of Matrix Chemical Structure on the Mode I and II Interlaminar Fracture Toughness of Glass-Fiber/Epoxy Composites

VERA ÁLVAREZ, CELINA R. BERNAL, PATRICIA M. FRONTINI, *and* ANALIA VÁZQUEZ*

Research Institute of Material Science and Technology (INTEMA)
Engineering Faculty, National University of Mar del Plata, Argentina
Juan B. Justo 4302 (7600) Mar del Plata, Argentina

The present paper is concerned with Mode I and Mode II delamination tests performed on three different glass fiber reinforced epoxy composites, chosen to obtain different final structures. The effect of crosshead speed on the fracture resistance of the composites was also analyzed. It was found that Mode I propagation values (G_{IC}) increase as the crosshead speed decreases, probably because of the increase of brittleness in the studied range. An Arrhenius type relation between G_{IC} and the glass transition temperature of the epoxy resin/amine system (T_g) was found. Mode II initiation values (G_{IIC}^{init}) and apparent shear strength (S_H) were found to increase with the decrease of T_g. The relation between matrix toughness and composite interlaminar fracture toughness was also considered. Finally, the G_{IC} propagation values were compared to the data available in literature for similar materials.

INTRODUCTION

A tough material is a material that requires greater stress or energy levels to reach a given failure point. Of the many factors to be considered in designing a tough fiber-reinforced composite, the first is the use of a tough base resin. Tougher epoxy resins can be obtained by decreasing the backbone stiffness, reducing the crosslink density, or by adding rubber modifiers (1, 2). An increase in fracture toughness with the decrease in crosslink density at a given temperature was found to be related to the change in glass transition temperature.

Fracture in epoxy resins is most likely rate-limited by chain scission. Chain scission depends on the axial stress that may develop in individual molecules. The crack-tip shear strain magnitude necessary to develop sufficient stress in individual molecules for chain scission to proceed depends on both, the crosslink density and the resin viscosity. When the resin viscosity is low, shear deformation can be produced before the chain scission takes place. The shear strain required to give a molecular stress sufficient to allow chain scission decreases as the molecular weight between crosslink decreases (3).

Delamination is one of the main failure modes for fiber reinforced polymer composites as it leads to a loss of stiffness or even complete fracture of the material (4, 5). Therefore, the resistance to delamination is one of the most important measured mechanical properties, and several test procedures for interlaminar fracture toughness characterization have been proposed (5, 6). The most commonly used test is the Mode I or opening test, using the double cantilever beam (DCB). An initial defect is produced and the Mode I interlaminar fracture toughness, G_{IC}, is determined as a function of the crack growth, by applying a constant displacement rate at the load points and measuring the load during the crack growth (5). The growth is usually stable, so it is possible to measure crack opening displacement (δ), load (P), and crack length (a) simultaneously when the displacement rate is slow. Another possibility is the use of Mode II interlaminar fracture toughness, G_{IIC}, to characterize the delamination resistance (5). The initial value of G_{IIC} is determined as a function of the P and δ values at which delamination starts.

The purpose of this work is to study the relation between the chemical structure of the resin and the mechanical properties of the resin-glass fiber composites. To this end, three types of diepoxy resins (aliphatic, cycloaliphatic, and aromatic) were chosen, and crosslinked with the same amine, to obtain different

*To whom correspondence should be addressed.
E-mail: anvazque@fi.mdp.edu.ar

backbone structures. A mixture of these epoxies is commonly used as a matrix in commercial composite preparation, in order to reduce the initial viscosity for impregnation (7).

In this study Mode I and Mode II delamination tests were employed, along with a short beam shear test. The sensitivity of each test to the change in chemical structure was also studied.

EXPERIMENTAL

Materials

Three different epoxies were used as matrices: an aromatic epoxy, diglycidylether of bisphenol A (Araldite® GY250), a cycloaliphatic epoxy (CY184), and an aliphatic epoxy, 1,4-butanediol diglycidylether (DGEBD). A primary diamine, (3DCM) was used as a curing agent. The stoichiometric ratio of aminohydrogen-to-epoxy was kept equal to 1. The chemical structures of the reagents are shown in *Table 1*. For each resin, the glass transition temperature and density were determined from D.S.C. measurements and picnometry, respectively.

Prepreg Preparation

A prepreg of each resin was prepared. In this way, a constant fiber content close to 60 vol% was obtained in the composites and the study of the delamination behavior could be done with reduced fiber bridging effects. Prepregs were prepared by impregnating a 120 mm × 140 mm unidirectional glass fiber mat (479 gr/m^2 surface density) with the epoxy-amine systems. Gel conversion of the system, x_{gel}, was calculated by means of the following equation (8):

$$x_{gel} = [(f - 1)\cdot(g - 1)]^{-0.5} \quad (1)$$

where f is the functionality of the epoxy groups and g is the functionality of hydrogen in the amine system. In the present case, epoxy functionality is 2 and amine functionality is 4. Consequently, the theoretical gel conversion is 0.577. In order to prepare a prepreg the reaction was stopped before completing, at a conversion value close to 0.4 (*Table 2*). The total heat of reaction was determined by means of D.S.C. on a Mettler-7 equipment at a heating rate of 10°C/min under nitrogen atmosphere.

Composite Preparation

For both Mode I and Mode II fracture toughness tests, three plies of prepregs were stacked in the zero direction. A non-adherent film of 40 μm thickness was inserted to introduce an artificial mid-plane crack and another three plies were added in the zero direction.

Table 1. Description of the Chemical Reagents.

Commercial name	Formula	Equivalent weight (g)
GY 250	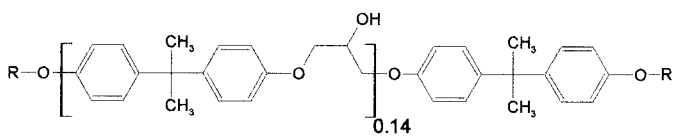	189.5
CY 184	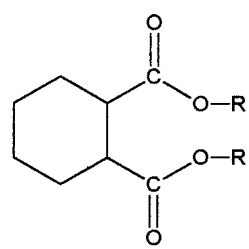	160.5
DGEBD	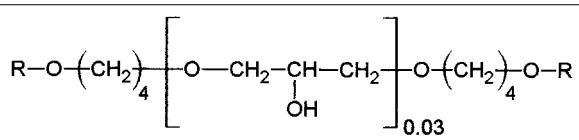	114.7
3DCM	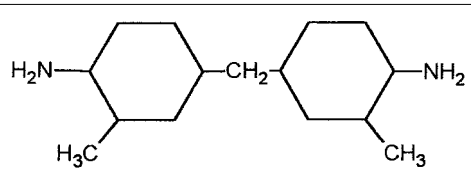	59.5

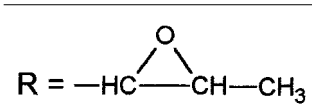

Table 2. Precuring Temperatures and Times to Produce the Prepregs.

System	Temperature (°C)	Time (hours)	Conversion
GY 250 + 3DCM	80	2	0.385
CY 184 + 3 DCM	60	1.5	0.377
DGEBD + 3DCM	50	1	0.391

The unidirectional panel was cured in a thermomechanical press (2.14 MPa) using the curing cycles shown in *Fig. 1* and *Table 3*. Then, the panel was postcured in an oven for 2 hours at 180°C. Full cure of the samples was verified by means of D.S.C. After curing, all laminates were cut parallel to the fiber direction using a diamond cutter, with a specimen thickness of 4 mm. Glass fiber content was determined by weighing the residue after burning off the resin, as explained elsewhere (9).

Mechanical Characterization of Matrices

Three-point bending tests were carried out at room temperature in order to determine the Young's moduli of the matrices following ASTM D790 recommendations. Fracture characterization of the matrices was carried out on three-point bend specimens of 5-mm thickness according to ASTM D 5045-93 at a crosshead displacement rate of 2 mm/min. Thickness-to-depth ratio (B/W) and span-to-depth ratio (S/W) were kept equal to 0.5 and 4, respectively. Central V notches

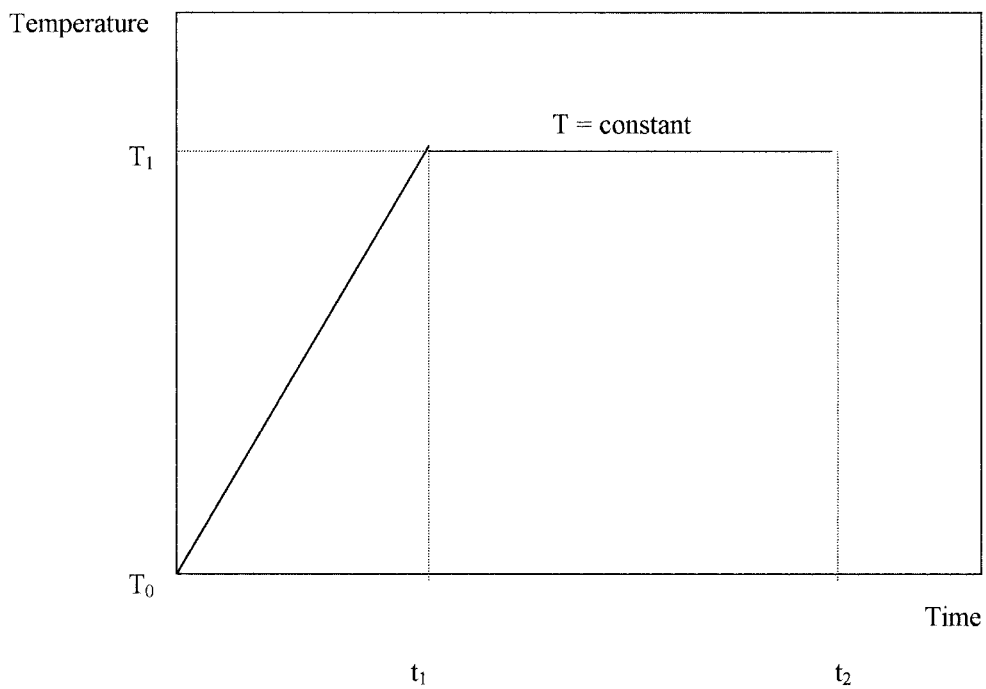

t_1 : time to reach the constant temperature used in the resin curing.
$t_2 - t_1$: time used to cure the resin at constant temperature.

Fig. 1. Curing cycles used for specimen preparation.

Table 3. Temperature-Time Cycles for Specimen Preparation (T_0 = 25°C).

System	t_1 (minutes)	T_1 (°C)	t_2-t_1 (minutes)
GY 250 + 3DCM	30	110	20
CY 184 + 3DCM	22	80	14
DGEBD + 3DCM	17	60	11

t_1: time to reach constant temperature used in the resin curing.
t_2-t_1: time used to cure the resin at constant temperature.

were machined in the bars and extended by tapping a fresh razor blade into the tip of the notch to give a crack length range of $0.45 < a/W < 0.55$. The length of the initial crack, a, was measured from the fracture surface using a profile projector (10×).

Plane strain fracture energy G_{IC} was calculated from the critical stress intensity factor as:

$$G_{IC} = \left(\frac{K_{IC}^2}{E}\right)(1 - \nu^2) \quad (2)$$

where ν is the Poisson's ratio of the material (ν = 0.35), E is the Young's modulus of the material measured at room temperature, and K_{IC} is the stress intensity factor at fracture initiation, calculated as:

$$K_{IC} = P_Q.(B.W)^{1/2}.f(a/W) \quad (3)$$

where P_Q is the load at break, B is the specimen thickness, W is the width of the specimen, a is the crack length, and $f(a/W)$ is a shape factor.

Uniaxial compression tests were also conducted on 10-mm-diameter cylindrical bars at a crosshead speed of 2 mm/min. Length-to-diameter ratio was 1.5. Specimens were machined to reach the final dimensions and improve edge surface finishing. The actual displacement was continuously recorded with a LVDT device. The compressive yield strength of each resin was taken as the maximum in the true stress−true strain curve.

All experiments were carried out at room temperature in a Shimadzu Autograph S-500-C Universal Testing Machine.

Mechanical Characterization of Composites

Double-cantilever beam specimens (DCB) were used for Mode I tests. Loads were applied through aluminum end blocks bonded to the specimens. A continuous loading crosshead speed between 1 and 5 mm/min was applied according to the ESIS Protocol for Interlaminar Fracture Testing of Composites (5). Crack lengths were observed on the specimen edge with the help of a layer of white paint and a video camera. Three tests were performed for each condition.

For Mode II tests, end-notched flexure specimens (ENF) were used. The loading rate was 1 mm/min. The real crack length-to-half span ratio (a/L) was always kept equal to 0.5. The dimensions used in this investigation are shown in *Table 4*.

The short-beam shear test was performed following the ASTM D2344-84 standard procedure. The span-to-thickness ratio ($2L/2h$) was kept equal to 5, the length-to-thickness ratio ($l/2h$) was between 7 and 8, and the crosshead speed was 1.3 mm/min.

RESULTS AND DISCUSSION

Matrix Behavior

Each resin in the study had a different chemical structure and therefore the network formed was also different. The characterization of the base matrix was done by means of picnometry, modulus, T_g and fracture toughness value. The density of each specimen was determined and it is shown in *Table 5*. Higher density samples could be correlated with higher crosslink density, which leads to samples with higher glass transition temperatures (10). The chemical structure of the aliphatic epoxy, DGEBD, has greater mobility of the chain between the crosslink points than the bisphenol A epoxy resin, GY250, resulting in an increase of the free volume.

As can be observed in *Table 5*, no significant differences between Young's moduli of the networks were found in this study. Similar results have been reported in literature (11). On the other hand, the expected decrease in compressive yield strength values with decreasing resin glass transition temperature was found (11).

Composite Behavior

Mode I Measurements

Mode I measurements of load, P, crack opening displacement, δ, and crack length, a, were converted to G_{IC} values by means of a modified beam theory expression (5). The modified beam theory requires the determination of a correction factor, Δ, to the crack

Table 4. Specimen Dimensions for the Different Tests Conducted on Composites.

Test	Length (l) mm	Width (W) mm	Thickness ($2h$) mm	Crack length (a) mm	Span ($2L$) mm
Mode I	120	20	4	45	—
Mode II	120	20	4	25	100
Short-Beam	32	20	4	—	22

Table 5. Properties of Matrix and Composites.

Epoxy	T_g (°C)	ρ (Kg/m^3)	σ_y^m (MPa)	E^m (GPa)	G_{IC}^m (J/m^2)	G_{IC}^c (J/m^2)	$G^{init}_{IIC}{}^c$ (J/m^2)	S_H^c (MPa)
GY 250	155	1200 ± 50	112.5 ± 1.5	2.49 ± 0.06	156 ± 12	115 ± 2	720 ± 12	39 ± 0.6
CY 184	102	1130 ± 40	88.5 ± 0.5	2.39 ± 0.07	214 ± 18	125 ± 1	768 ± 15	43 ± 0.7
DGEBD	66	1080 ± 50	59.5 ± 1.0	2.46 ± 0.09	985 ± 32	142 ± 4	824 ± 17	46 ± 0.5

length to account for crack-tip rotation and shear deformation. This correction is obtained by plotting compliance ($C = \delta/P$) to the one-third power, against crack length. The correction factor, Δ, is the intercept on the x-axis (*Fig. 2*). Then, the interlaminar fracture toughness is computed as:

$$G_{IC} = \frac{3.P.\delta}{2.W.(a + \Delta)} \tag{4}$$

where W is the specimen width.

The modified beam theory allows Young's modulus E to be determined for the material, which is a useful check on the procedure (5)

$$E = \frac{8.(a + \Delta)^3}{C.W.h^3} \tag{5}$$

where h is the thickness of one arm of the specimen. The value of E must be independent of crack length.

For glass reinforced GY-250 epoxy resin, the test was done at three different loading rates: 2, 3.5 and 5 mm/min. Results are shown in *Fig. 3*. Even though the displacement rate was moderately changed, the G_{IC} values decreased as the loading rate increased in the studied range. This may be due to an increase in brittleness of the matrix with increasing loading rate (12).

In *Fig. 4a*, *b* and *c*, propagation values of G_{IC} for different glass reinforced epoxies at a loading rate of 2 mm/min are shown. The results were determined from the modified beam theory analysis, as stated before. The value of G_{IC} appears constant with increasing crack length. This result is consistent with the fact that there is no evidence of fiber bridging behind the advancing crack tip (13) and also consistent with the results reported in literature for similar epoxy composites (14). *Figure 5* shows the fracture surface of a specimen tested in Mode I. No broken fibers were found, which is indicative of the absence of fiber bridging (13).

The load versus displacement curves for the composites tested are shown in *Fig. 6*. For the aromatic epoxy, GY250, the curve is linear during crack growth. The cycloaliphatic epoxy, CY184, and aliphatic epoxy, DGEBD, have similar behavior. After initiation of the crack, there is first a stable propagation and then a clear tendency for unstable, "stick-slip" crack growth. The deviation from linearity of the initial slope of the load versus displacement curve is associated with stable crack growth. The stable cracking followed by rapid crack growth leads to crack arrest. However, the cycloaliphatic resin displays a lower crack velocity than the aliphatic one. Frassine *et al.* (15) have observed unstable crack propagation with stick-slip behavior when the test temperature decreases for this kind of epoxy resin (that is, when the resin is in the glassy state). The same behavior could be obtained with an increase of the T_g value and the same test temperature.

The influence of the matrix on Mode I propagation values is shown in *Table 5*. A decrease of G_{IC} propagation values with increasing glass transition temperature

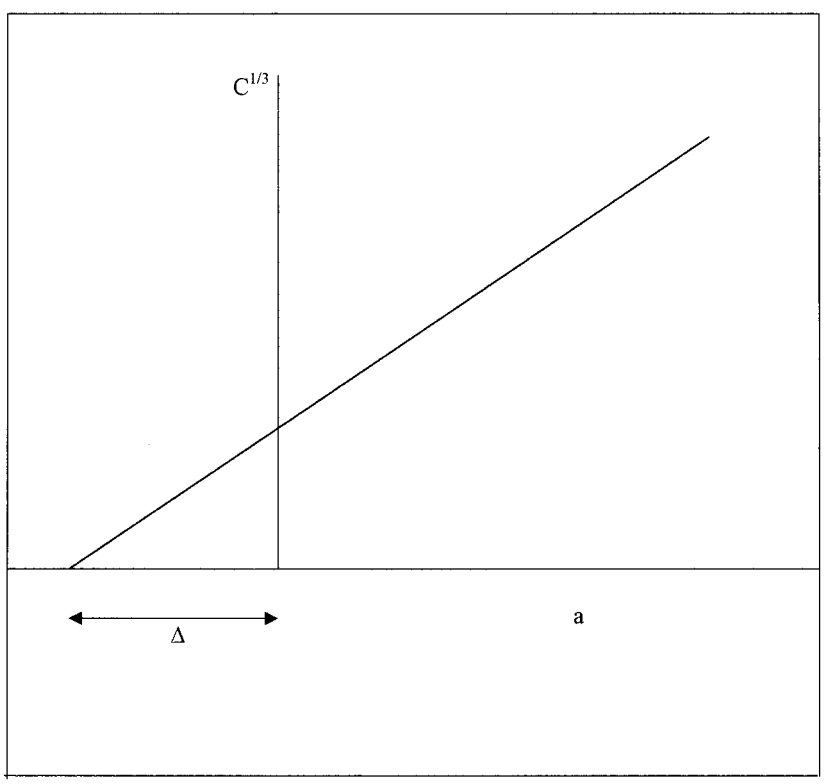

Fig. 2. Determination of correction factor, Δ.

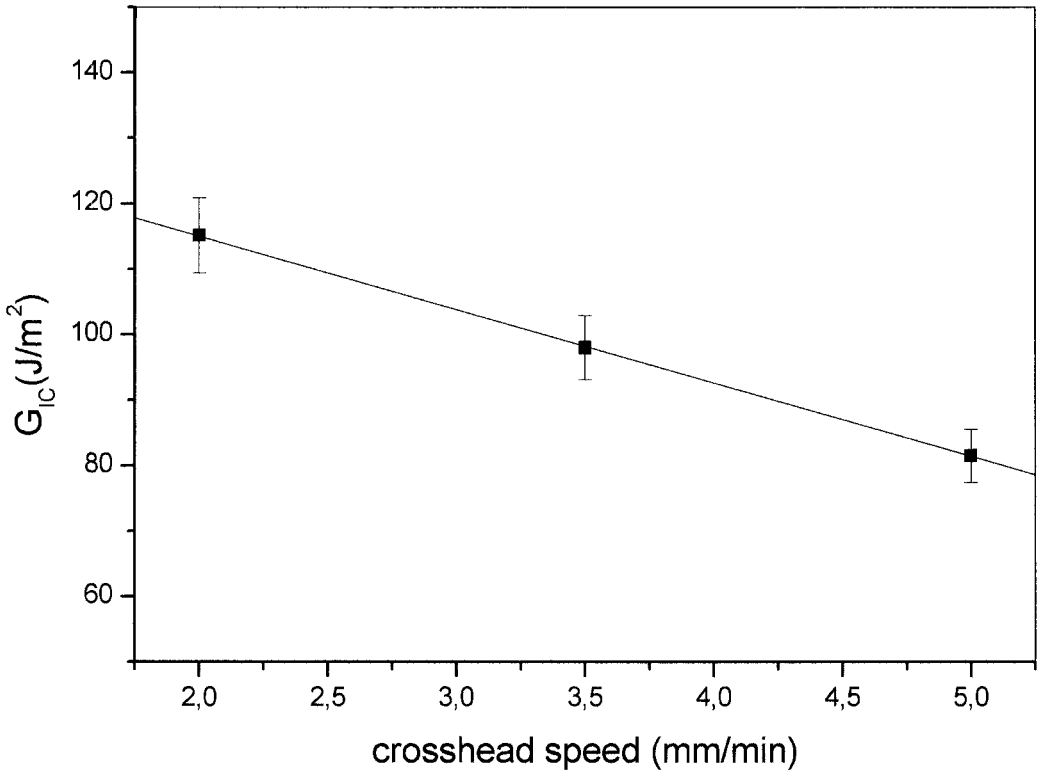

Fig. 3. Influence of crosshead speed on G_{IC} propagation values.

of the epoxy/amine system was observed, probably due to the lower capability of the matrix of developing crack-tip shear deformation at greater differences between the test temperature and the glass transition temperature (1). A similar trend was reported in the literature for un-reinforced epoxy resins, in the same range of relative temperatures (2).

G_{IC} was found to be related to the glass transition temperature of the matrix (T_g) by the following equation:

$$G_{IC} = C_1.e^{C_2/(T_g - T)} \tag{6}$$

By plotting the natural logarithm of G_{IC} against $1/(T_g - T)$ the values of the parameters C_1 and C_2 were determined (*Fig. 7*). They are C_1 = 105.3°C and C_2 = 12.4 J/m^2. This relation between G_{IC} and T_g is very useful in predicting the interlaminar fracture toughness for systems with known glass transition temperature.

Mode I propagation values obtained in this investigation were also contrasted to bibliographic data for similar materials (16) and a reasonable agreement was found. The matrix G_{IC} value ($G_{IC}{}^m$) has a greater value than the composite G_{IC} value ($G_{IC}{}^c$) in contrast to the results reported for brittle matrix composites (17, 18). The absence of fiber bridging that otherwise would contribute to the energy dissipation in these brittle matrix composites could be partially responsible for this behavior. In the present case, the rate of increase is steeper for $G_{IC}{}^m$ than for $G_{IC}{}^c$ as expected for ductile matrices. The deformation zone increases as the system goes from aromatic to aliphatic epoxy. The deformation zone extends several fiber diameters beyond the resin-rich region between plies. The amount of resin ductility controls the degree of crack tip blunting, which in combination with the stress redistribution due to non-linear deformation determines the resistance to crack extension. It is clearly shown that the resin with aliphatic epoxy has the largest differences between $G_{IC}{}^m$ and $G_{IC}{}^c$. This is in agreement with the results reported in literature for a carbon-epoxy system with a fiber volume fraction of 58% and a ductile epoxy resin (17).

Mode II Measurements

Mode II interlaminar fracture toughness values (G_{IIC}) were determined from the load-displacement measurements and the initial crack length by using the corrected beam theory equation:

$$G_{IIC} = \frac{9.P^2.a^2}{16.W^2.E_F.h^3} \tag{7}$$

where E_F is the flexural modulus with a equal to 0. This modulus was determined according the ASTM D790-93 recommendations. The test was stopped when the load, P, begins to decrease. *Table 5* shows the initiation values of G_{IIC} ($G_{IIC}{}^{init}$) for the three epoxies used

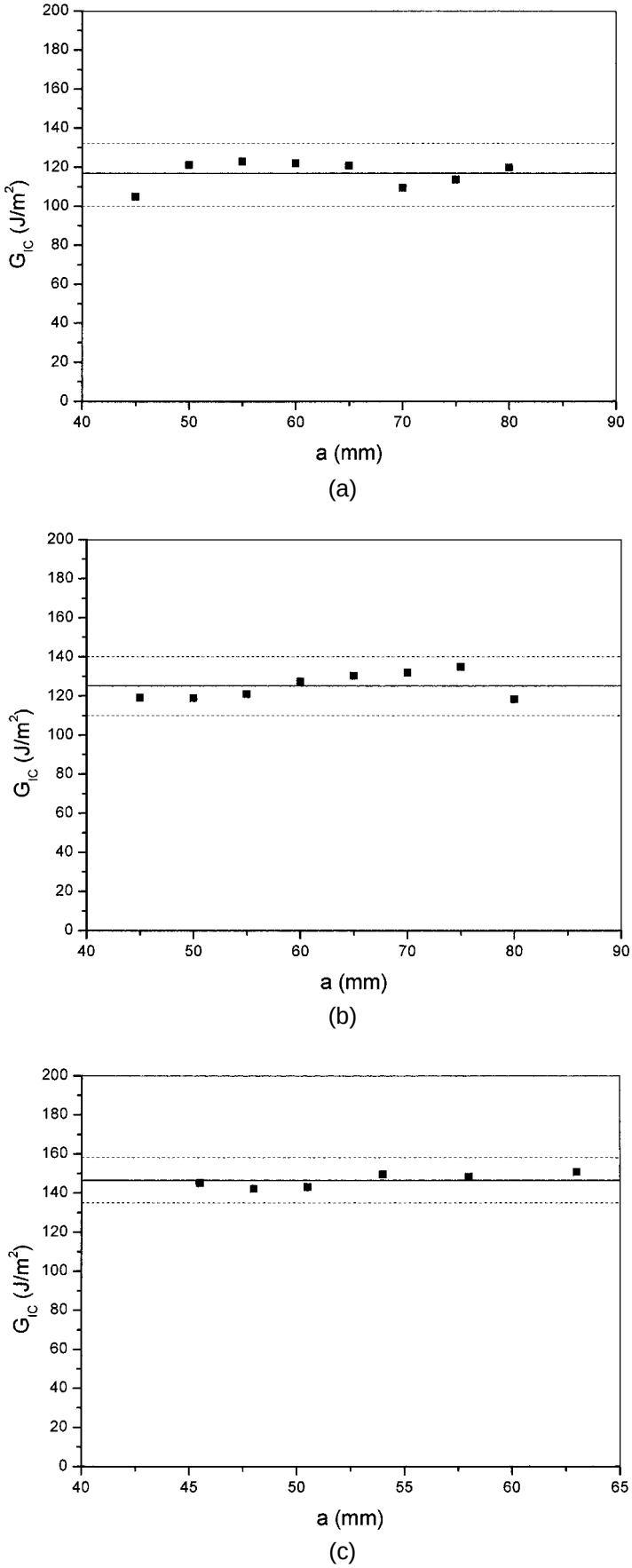

Fig. 4. G_{IC}^{c} propagation values for different chemical epoxy systems: a) GY250, b) CY184 and c) DGEBD.

Fig. 5. Optical microphotography of the fractured surface.

for the composites. In this case, G_{IIC}^{init} increases as T_g decreases as in Mode I, but an Arrhenius relationship between G_{IIC}^{init} and T_g, as in *Eq 6*, could not be established. The value of G_{IC} was lower than the value of G_{IIC}^{init}, in agreement with the literature (17−19).

Short-Beam Shear Tests

To determine the apparent shear strength, S_H, the following equation was used:

$$S_H = \frac{0.75.P_f}{W.B} \tag{8}$$

where P_f is the load that produces the specimen failure, and B and W, are sample thickness and width respectively. The results for the short-beam test are shown in *Table 5*. The apparent shear strength increases as T_g decreases in agreement with the results of Mode I and Mode II delamination tests.

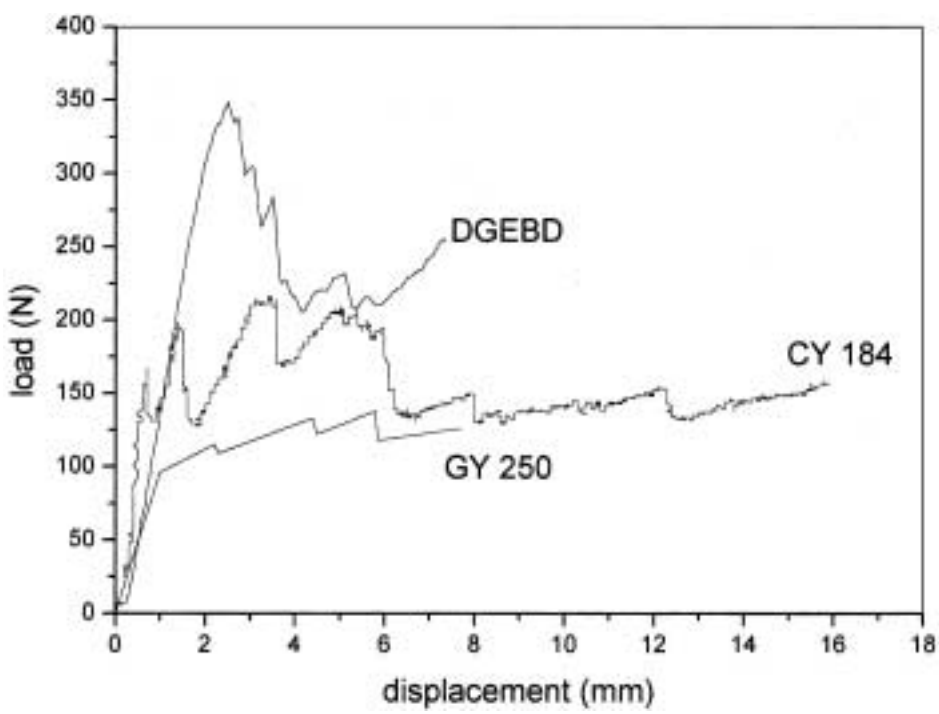

Fig. 6. Typical load versus displacement curves for different epoxy composites.

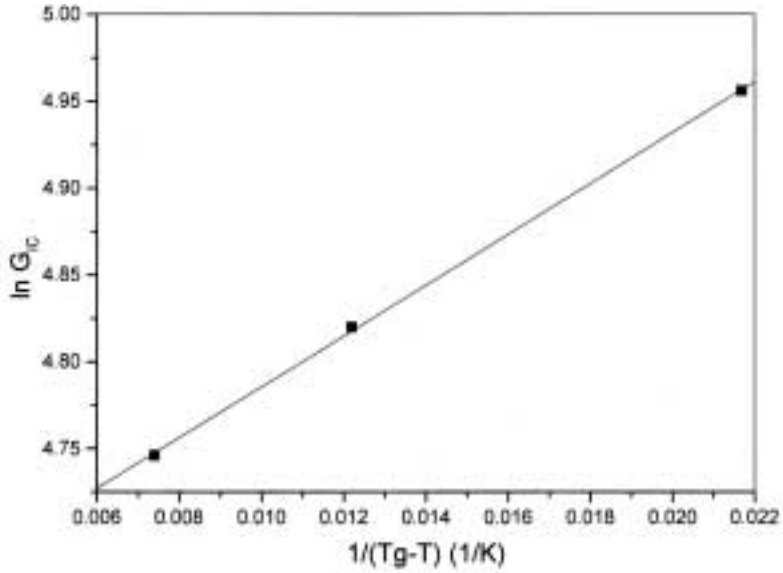

Fig. 7. Relationship between G_{IC}^c and T_g values.

CONCLUSIONS

A relation between chemical structure and mechanical properties for glass/fiber epoxy composites was found using three different epoxy systems. The different chemical structures of the resins allow us to compare different densities and glass transition temperatures. An Arrhenius type exponential dependence for the fracture toughness in Mode I and the glass transition temperature of the resins was found. The toughest composite was obtained with the resin with the lowest difference between the test temperature and the glass transition temperature.

Interlaminar fracture evaluation by means of Mode II produces higher sensitivity in the differences than Mode I measurements. This result and the greater experimental simplicity of Mode II measurements make this method more appealing than Mode I for characterizing the interlaminar fracture toughness of these glass-fiber/epoxy composites.

On the other hand, the results of short-beam shear tests have the same trend as Mode I and II, but that method has the advantage of being the easiest to implement among the three methods.

ACKNOWLEDGMENTS

We appreciate the financial support provided by Fundación Antorchas and the National Research Council of Argentina (CONICET).

REFERENCES

1. W. L. Bradley, W. Schultz, C. Corleto, and S. Komatsu, *Toughened Plastics*, C. Keith Riew and A. J. Kinloch, eds., Advances in Chemistry Series 233, p. 317, American Chemical Society (1993).
2. J. Galy, J. F. Gérard, H. Sautereau, R. Frassine, and A. Pavan, *Polym. Network Blends*, 4, 105 (1994).
3. B. Burton and J. L. Bertram, *Polymer Toughening*, p. 334, Charles Arends, ed., Marcel Dekker, New York (1996).
4. S. Hashemi, A. J. Kinloch, and J. G. Williams, *Proc. Roy. Soc. London*, A427, 173 (1990).
5. P. Davies, *Protocols for interlaminar fracture testing composites*, European Structural Integrity Society, Polymers and Composites Task Group, France (1988–1996).
6. J. W. Gillespie and D. A. Carlsson, *Delaware Encyclopedia of Composite Materials*, Vol. 6, p. 111, Technomic Publishing, Lancaster, Pa. (1990).
7. B. Ellis, *Chemistry and Technology of Epoxy Resins*, Chapman and Hall, London (1993).
8. J. P. Flory, *Principles of Polymer Chemistry*, p. 347, Cornell University Press, Ithaca, N.Y. (1953).
9. M. H. Geier, *Quality Handbook for Composite Materials*, p. 171, Chapman and Hall, London (1994).
10. C. I. Vallo, P. M. Frontini, and R. J. J. Williams, *Polymer Gels and Networks*, 1, 257 (1993).
11. E. D. Crawford and A. J. Lesser, *Polym. Eng. Sci.*, 39, 385 (1999).
12. R. S. Kody and S. J. Lesser, *J. Mat. Sci.*, 32, 5637 (1997).
13. I. N. Dyson, A. J. Kinloch, and A. Okada, *Composites*, 25, 189 (1994).
14. H. You and Y-J. Yum, *J. Reinf. Plast. Composites*, 16 (6), 537 (1997).
15. R. Frassine, M. Rink, and A. Pavan, *Comp. Sci. Tech.*, 56, 1 (1996).
16. P. Krawcsak and J. Pabiot, *J. Comp. Mat.*, 29, 2230 (1995).
17. J-K. Kim and Y-W. Mai, *Engineered Interfaces in Fiber Reinforced Composites*, p. 43, Elsevier, New York (1998).
18. W. M. Jordan, W. L. Bradley, and R. J. Moulton, *J. Comp. Mat.*, 23, 923 (1989).
19. R. Rikards, A. Korjakin, F. G. Buchholz, H. Wang, A. K. Bledzki, and G. Wacker, *J. Comp. Mat.*, 32, 1528 (1988).